Murine tissue factor disulfide mutation causes a bleeding phenotype with sex specific organ pathology and lethality

Sluka, Susanna H M ; Stämpfli, Simon F ; Akhmedov, Alexander ; Klein-Rodewald, Tanja ; Sanz-Moreno, Adrián ; Horsch, Marion ; Grest, Paula ; Rothmeier, Andrea S ; Rathkolb, Birgit ; Schrewe, Anja ; Beckers, Johannes ; Neff, Frauke ; Wolf, Eckhard ; Camici, Giovanni G ; Fuchs, Helmut ; Gailus-Durner, Valerie ; Hrabě de Angelis, Martin ; Lüscher, Thomas F ; Ruf, Wolfram ; Tanner, Felix C

Abstract: Tissue factor is highly expressed in sub-endothelial tissue. The extracellular allosteric disulfide bond Cys186-Cys209 of human tissue factor shows high evolutionary conservation and in vitro evidence suggests that it significantly contributes to tissue factor procoagulant activity. To investigate the role of this allosteric disulfide bond in vivo, we generated a C213G mutant tissue factor mouse by replacing Cys213 of the corresponding disulfide Cys190-Cys213 in murine tissue factor. A bleeding phenotype was prominent in homozygous C213G tissue factor mice. Pre-natal lethality of 1/3rd of homozygous offspring was observed between E9.5 and E14.5 associated with placental hemorrhages. After birth, homozygous mice suffered from bleedings in different organs and reduced survival. Homozygous C213G tissue factor male mice showed higher incidence of lung bleedings and lower survival rates than females. In both sexes, C213G mutation evoked a reduced protein expression (about 10-fold) and severely reduced pro-coagulant activity (about 1000-fold). Protein glycosylation was impaired and cell membrane exposure decreased in macrophages in vivo. Single housing of homozygous C213G tissue factor males reduced the occurrence of severe bleeding and significantly improved survival, suggesting that inter-male aggressiveness might significantly account for the sex differences. These experiments show that the tissue factor allosteric disulfide bond is of crucial importance for normal in vivo expression, post-translational processing and activity of murine tissue factor. Although C213G tissue factor mice do not display the severe embryonic lethality of tissue factor knock-out mice, their postnatal bleeding phenotype emphasizes the importance of fully functional tissue factor for hemostasis.

DOI: https://doi.org/10.3324/haematol.2019.218818

factor disulfide mutation causes a bleeding phenotype with sex specific organ pathology and lethality. Haematologica, 105(10):2484-2495.
DOI: https://doi.org/10.3324/haematol.2019.218818

haematologica
Journal of The Ferrata Storti Foundation

Murine tissue factor disulfide mutation causes a bleeding phenotype with sex specific organ pathology and lethality

by Susanna H. M. Sluka, Simon F. Stämpfli, Alexander Akhmedov, Tanja Klein-Rodewald, Adrián Sanz-Moreno, Marion Horsch, Paula Grest, Andrea S. Rothmeier, Birgit Rathkolb, Anja Schrewe, Johannes Beckers, Frauke Neff, Eckhard Wolf, Giovanni G. Camici, Helmut Fuchs, Valerie Gailus-Durner, Martin Hrabě de Angelis, Thomas F. Lüscher, Wolfram Ruf, and Felix C. Tanner

Haematologica 2019 [Epub ahead of print]

Citation: Susanna H. M. Sluka, Simon F. Stämpfli, Alexander Akhmedov, Tanja Klein-Rodewald, Adrián Sanz-Moreno, Marion Horsch, Paula Grest, Andrea S. Rothmeier, Birgit Rathkolb, Anja Schrewe, Johannes Beckers, Frauke Neff, Eckhard Wolf, Giovanni G. Camici, Helmut Fuchs, Valerie Gailus-Durner, Martin Hrab de Angelis, Thomas F. Lüscher, Wolfram Ruf, and Felix C. Tanner. Murine tissue factor disulfide mutation causes a bleeding phenotype with sex specific organ pathology and lethality.
Haematologica. 2019; 104:xxx
doi:10.3324/haematol.2019.218818

Murine tissue factor disulfide mutation causes a bleeding phenotype with sex specific organ pathology and lethality

Susanna H. M. Sluka[1]*, Simon F. Stämpfli[1,2,3]*, Alexander Akhmedov[1], Tanja Klein-Rodewald[4], Adrián Sanz-Moreno[4], Marion Horsch[4], Paula Grest[5], Andrea S. Rothmeier[6], Birgit Rathkolb[4,7,8], Anja Schrewe[4], Johannes Beckers[4,8,9], Frauke Neff[4], Eckhard Wolf[7], Giovanni G. Camici[1], Helmut Fuchs[4], Valerie Gailus-Durner[4], Martin Hrabě de Angelis[4,8,9], Thomas F. Lüscher[1,2], Wolfram Ruf[6,10], and Felix C. Tanner[1,2]

**SHMS and SFS contributed equally to this work*

[1] Center for Molecular Cardiology, University of Zurich, Zurich, Switzerland
[2] Department of Cardiology, University Heart Center, University Hospital, Zurich, Switzerland
[3] Cardiology Division, Heart Center, Luzerner Kantonsspital, Luzern, Switzerland
[4] German Mouse Clinic, Institute of Experimental Genetics, Helmholtz Zentrum München, German Research Center for Environmental Health, Neuherberg, Germany
[5] Institute of Veterinary Pathology, University of Zurich, Zurich, Switzerland
[6] Department of Immunology and Microbiology, Scripps Research, La Jolla, CA, USA
[7] Institute of Molecular Animal Breeding and Biotechnology, Gene Center, Ludwig-Maximilians-University München, Munich, Germany
[8] German Center for Diabetes Research (DZD), Neuherberg, Germany
[9] Experimental Genetics, School of Life Science Weihenstephan, Technische Universität München, Freising, Germany
[10] Center for Thrombosis and Hemostasis Johannes Gutenberg University Medical Center, Mainz, Germany

Address for correspondence:
Felix C. Tanner, MD, Cardiology, University Heart Center Zurich, Rämistrasse 100, CH-8091 Zurich, Switzerland, Phone +41 44 255 99 97, Fax +41 44 255 49 04, Email: felix.tanner@usz.ch

Abstract

Tissue factor is highly expressed in sub-endothelial tissue. The extracellular allosteric disulfide bond Cys186–Cys209 of human tissue factor shows high evolutionary conservation and in vitro evidence suggests that it significantly contributes to tissue factor procoagulant activity.

To investigate the role of this allosteric disulfide bond in vivo, we generated a C213G mutant tissue factor mouse by replacing Cys213 of the corresponding disulfide Cys190-Cys213 in murine tissue factor.

A bleeding phenotype was prominent in homozygous C213G tissue factor mice. Pre-natal lethality of 1/3rd of homozygous offspring was observed between E9.5 and E14.5 associated with placental hemorrhages. After birth, homozygous mice suffered from bleedings in different organs and reduced survival. Homozygous C213G tissue factor male mice showed higher incidence of lung bleedings and lower survival rates than females. In both sexes, C213G mutation evoked a reduced protein expression (about 10-fold) and severely reduced pro-coagulant activity (at least 100-fold). Protein glycosylation was impaired and cell membrane exposure decreased in macrophages in vivo. Single housing of homozygous C213G tissue factor males reduced the occurrence of severe bleeding and significantly improved survival, suggesting that inter-male aggressiveness might significantly account for the sex differences.

These experiments show that the tissue factor allosteric disulfide bond is of crucial importance for normal in vivo expression, post-translational processing and activity of murine tissue factor. Although C213G tissue factor mice do not display the severe embryonic lethality of tissue factor knock-out mice, their postnatal bleeding phenotype emphasizes the importance of fully functional tissue factor for hemostasis.

Introduction

Tissue factor (TF) is the cellular activator of the extrinsic pathway of blood coagulation. It is expressed in the sub-endothelial wall of blood vessels and organ parenchyma, leading to activation of coagulation after vessel injury. Levels of TF expression, however, differ significantly between organs: heart, brain, lung, and uterus exhibit very high TF expression, while TF is barely detectable in skeletal muscle and joints [1, 2]. Total TF deletion in mice leads to embryonic death due to insufficient development of yolk sac vessels and vascular failure [3-5]. A TF transgene inducing low expression of human full length TF (flTF) in mice (low-TF mice, ~1% of normal murine TF levels) is sufficient to rescue TF knockout mice from embryonic lethality [6] but not to restore normal postnatal hemostatic function. These mice suffer from spontaneous hemorrhages particularly in organs which in wild-type mice express high levels of TF such as heart, lung, brain, gastrointestinal tract, and testis [7-9]. Fatal lung hemorrhages are very common in low-TF mice [8, 10] and are further enhanced when exposed to either intratracheal lipopolysaccharide [11] or infected with influenza A virus [12]. Similarly, fatal brain hemorrhages have been observed in low-TF mice [10]. Furthermore, female low-TF mice exhibit fatal hemorrhages in placenta and uterus during pregnancy and postpartum, suggesting that TF is crucial for uterine hemostasis [13]. In line with these observations, tail bleeding time in low-TF mice was increased [14].

Due to its sub-endothelial localization, TF is separated from circulating clotting factors in the absence of an injury. Minor amounts of TF are however expressed on the surface of monocytes and come in contact with blood [15, 16]. To control pro-coagulant activity, TF activity is post-translationally suppressed by a mechanism called encryption [17]. The mechanism of encryption is controversially discussed: several studies suppose that predominantly exposure of negatively charged phospholipids

account for the decryption of TF activity [18, 19], while others suggest activation via thiol disulfide exchange reactions [20-25] involving complement activation. Human TF indeed contains 2 disulfide bonds (Cys49-Cys57 and Cys186-Cys209) which are conserved in mice (Cys47-Cys55 and Cys190-Cys213) and many other species. The C-terminal bond shares sequence features of other allosteric disulfide bonds and is important for TF pro-coagulant activity [26] and thus crucial for regulation of TF activity in cell cultures [27, 28]. Release of pro-coagulant, TF-containing extracellular vesicles (EV) from bone marrow-derived macrophages (BMDM) and smooth muscle cells was shown to be regulated by ATP stimulation of the purinergic receptor P2X7 [29], also depending on thiol-exchange reactions [29].

We generated a C213G TF knock-in (KI) mouse model to investigate the function of disulfide bond mutated TF in vivo and its contribution to hemostasis.

Methods

Construction of the C213G TF targeting vector

The coding sequence of the murine full-length TF isoform containing a T721G mutation as well as the flanking genomic regions were inserted into KpnI/NotI restriction sites of a LNTK vector to replace the genomic TF locus. Embryonic stem cell transfection (129P2/OlaHsd) and blastocyst injection was conducted by PolyGene (Ruemlang, Switzerland). Chimeric mice were bred with C57BL/6J mice.

Animals

One mouse colony was bred of heterozygous animals on a mixed 129P2/OlaHsd-C57BL/6J background (50% from each strain). Mice were backcrossed to C57BL/6J (B6). All tests performed were approved by the responsible authority of the local government.

Embryonic analysis

For embryonic analyses heterozygous C213G/+ TF mice were bred and females were controlled for plugs every morning (day of the plugs considered E0.5).

Pathological analysis

All organs were fixed in 4% buffered formalin and embedded in paraffin for histological examination. Four-µm-thick sections were cut and stained.

Expression profiling

Total RNA was isolated from organs just before microarray hybridization. Amplified RNA was hybridized and analyzed on Illumina MouseRef8 v2.0 Expression Bead Chips containing about 25K probes.

Bleeding time

After onset of anesthesia, tails were prewarmed in a 37°C water bath for 10 min. Then 0.5 mm of the tail tip was amputated, and the tail was immediately put back to 37°C PBS.

Tail-cuff blood pressure measurement

Blood pressure was measured in non-anesthetized mice with a non-invasive tail-cuff method using the MC4000 Blood Pressure Analysis Systems.

TF expression analysis

RNA was extracted using TRIzol Reagent (Molecular Research Center). Transcript levels were quantified by Real Time PCR using SyBr Green Master Mix on an Applied Biosystems 7300 System. Protein was extracted by grinding of organ tissue in lysis buffer. Samples were separated by 10% SDS-PAGE and transferred to a PVDF membrane (Immobilion®-FL, Millipore). The membrane was stained with anti-mouse TF rabbit antiserum (R8084) [29] and anti-human GAPDH (cross-reactive to mouse) mouse monoclonal (MAB374, Millipore) primary antibodies, followed by secondary antibodies.

TF activity

Tissue was lysed in HEPES-saline containing 0.02% sodium azide (HBS) and diluted in HBS containing 1mg/ml BSA and 50 µM phospholipid vesicles to measure TF activity using a plasma clotting assay.

Macrophage experiments

Femora and tibiae were dissected and flushed with RPMI. Cells were resuspended in 90% FCS, 10% DMSO. Bone marrow-derived macrophages (BMDM) were generated from total bone marrow cell cultures as described previously [30]. Cell surface TF activity was determined with 0.5 nM FVIIa and 50 nM FX in HBS by measuring a time course of FXa generation. TF EV activity was measured in HBS with 2 nM VIIa and 100 nM FX. EV prothrombinase activity was measured in HBS with 10 nM FVa, 5 nM FXa and 500 nM prothrombin. RNA was isolated from macrophages using TRIzol Reagent. Transcript levels were quantified by Real Time PCR.

Statistical analyses

Data are indicated as mean ± SEM. Unpaired Student's t-test and two-way ANOVA were used as appropriate. For comparison of genotype distributions, a X^2-test was applied. A p value <0.05 was considered as significant.

Results

Generation of C213G TF KI mice

To generate mice expressing C213G TF under the control of the endogenous TF promoter, a replacement-type targeting vector was cloned. This vector contained the coding sequence of C213G full length TF, which was flanked by 3kb 5' and 5.2kb 3' arms of homology; thus, the endogenous TF sequence was replaced by the C213G TF coding sequence by homologous recombination (Figure 1A).

Partial developmental lethality in homozygous C213G TF offspring

Heterozygous mice were bred, and among 889 offspring on a C57BL/6J genetic background, 141 homozygous C213G/C213G (16.1%) TF, 508 heterozygous C213G/wt TF (57.5%), and 240 (26.4%) wt animals were found at weaning. At birth, among 320 offspring, 56 homozygous C213G/C213G (17.5%), 170 heterozygous C213G/wt (53.1%), and 94 wt (29.4%) were found, excluding significant post-natal lethality (Figure 1B). Thus, 1/3 of homozygous C213G/C213G pups were missing at birth and both genotype distributions at weaning and at birth differed significantly from a mendelian distribution.

Genetic deletion of the TF gene in mice leads to embryonic lethality between embryonic day (E) 9.5 and 10.5 [3]. To determine whether homozygous C213G/C213G TF embryos are generated at mendelian ratios, 70 E9.5 embryos on a B6 genetic background were genotyped. Eighteen homozygous C213G/C213G TF (25.7%), 34 heterozygous C213G/wt TF (48.6%), and 18 wt (25.7%) embryos were found, which goes along with mendelian segregation (Figure 1B). In contrast to TF KO mice, histology did not show any impairment of yolk sac vessel integrity and normal levels of α-SMA expression in homozygous C213G/C213G TF yolk sacs at E9.5

(Supplemental Figure 1A) [3]. At embryonic day 14.5, 11 vital homozygous C213G/C213G TF (16.4%), 34 heterozygous C213G/wt (50.8%) and 22 wt embryos (32.8%) were found, indicating that C213G/C213G TF mice show partial developmental lethality between day 9.5 and 14.5. Embryonic growth required umbilical blood flow via the chorioallantoic placenta from day 10.5 [31]. Besides the 11 vital homozygous C213G/C213G TF embryos, 3 necrotic homozygous embryos could be identified on day 14.5 showing retinal pigmentation which indicates development to at least E11.5 [32]. Additional resorbed implantation sites were present, which could not be genotyped. Placentas of both vital and necrotic homozygous C213G/C213G TF embryos showed hemorrhages of variable number and size (Supplemental Figure 1A).

Decreased survival of adult homozygous C213G/C213G TF offspring

Between the age of 3 to 4 weeks, about 10% homozygous C213G/C213G TF mice on B6 background developed a hydrocephalus, while this was not observed in C213G/C213G TF animals on a mixed background (data not shown). This may be due to the tendency of wt B6 mice to develop spontaneous hydrocephalous [33].
With progressing age some homozygous C213G/C213G TF mice developed symptoms of disease, mostly dyspnea, apathy and weight loss, but sometimes also neurological symptoms or spontaneous death. Diseased animals were euthanized when they met defined termination criteria. Both euthanized animals and those which died were included in the survival analysis. We found a sex difference in survival with impaired survival of male homozygous C213G/C213G TF mice. The sex difference was more pronounced in animals on a mixed background ($p<0.001$) compared to animals on a B6 background ($p=0.17$, Figure 1C). Dissection of dead and euthanized mice showed macroscopic bleedings to heart, lung, and brain, which are organs with

high TF expression. Hemorrhages were confirmed microscopically in heart, lung, and brain (Figure 2 A-D). They were accompanied by secondary changes like epi- and myocarditis and fibrosis in hearts as well as edema (Figure 3A-B), bronchiolitis obliterans, and pneumonia in lungs.

Sex difference in organ pathology

In order to quantify the incidence of organ bleedings, we analyzed a group of male and female homozygous C213G/C213G TF mice on a B6 background without apparent disease symptoms. This analysis of asymptomatic mice provided a measure for the incidence of organ bleedings in a uniform group of mice of both sexes of the same age. At 17 weeks of age we found a similar incidence of hemorrhages in heart (7/11 in females and 5/10 in males) and brain (2/11 in females and 2/10 in males) of male and female homozygous C213G/C213G TF mice, while the incidence of lung hemorrhage was more pronounced in males (5/10) as compared to females (1/11) (Supplemental Figure 1B). Lungs of male homozygous C213G/C213G TF mice also exhibited macroscopically more hemorrhagic areas in comparison to female mice and these were accompanied by edema in severe cases (Figure 2A). Histologically, affected areas showed intra-alveolar hemorrhage and the presence of macrophages, eosinophilic fibrillar material in bronchial lumen, and peri-vascular and peri-bronchial inflammatory infiltrates (Figure 2B). In contrast to reported calcified testes in low-TF mice [9], we did not observe calcification of testes (Supplemental Figure 2A).

Epi- and myocardial hemorrhages (Figure 2C) as well as inflammation representing myocarditis (Figure 3A) were observed in hearts of homozygous C213G/C213G TF mice. Furthermore, fibrotic changes were detectable in all hearts of homozygous C213G/C213G TF mice, even without acute hemorrhage or inflammation (Figure 3B).

However, blood pressure and heart rate of male and female C213G/C213G TF mice were comparable to that of male and female wt TF mice (Supplemental Fig. 2B).

Molecular changes in heart and lung of C213G/C213G TF mice

Using Illumina Bead array, we assessed gene expression profiles in hearts and lungs of male and female homozygous C213G/C213G TF mice compared to the mean expression values of wt TF mice (Figure 3C, Supplemental Table 1). 113 genes were significantly regulated in male and 178 genes in female C213G/C213G TF mouse hearts. GO-terms which were both overrepresented in hearts of homozygous male and female C213G/C213G TF mice were cellular movement, hematological system, immune cell trafficking, cancer, cardiovascular system, cellular growth and proliferation, skeletal and muscular disorders, cell-to-cell signaling and interaction, metabolic disease, cardiovascular disease, respiratory disease, and cell death. This is in line with inflammation and fibrotic remodeling. In male C213G/C213G TF mouse lungs 69 genes were significantly upregulated and classified to the following overrepresented GO terms: inflammatory response, cellular movement, cell-to-cell signaling, hematological system, connective tissue, cancer, respiratory disease, cardiovascular disease, and lipid metabolism. In contrast, in female C213G/C213G TF mouse lungs only 23 genes were weakly regulated (fold change of -3.66 to 2.10) while no GO term was overrepresented. Although the macroscopically least affected lungs were selected for the analysis, the differential gene regulation in male C213G/C213G TF lungs compared to females suggests increased early pathological alterations and supports the sex difference in lung pathology.

Tail bleeding time and blood cell counts

Tail bleeding was measured to investigate whether primary differences exist in hemostatic capacity. Tail bleeding time was prolonged in homozygous C213G/C213G TF mice of both sexes, but no difference was detected between the sexes (Figure 4A). Comparing blood counts of C213G/C213G TF mice to wt mice revealed a mild decrease of cellular hemoglobin content (MCH) and concentration (MCHC), slightly increased reticulocyte numbers with more immature reticulocytes, and an increased mean platelet size due to a higher proportion of big platelets (>12fl) in homozygous C213G/C213G TF mice (Figure 4B). Even though these findings are consistent with compensated chronic bleedings, the absolute change of the values was small.

TF expression and activity

TF mRNA expression was measured in heart, brain, and lung of male and female homozygous C213G/C213G TF and wt mice using flTF specific primers (Figure 5A). flTF expression was slightly elevated in brain and lung of homozygous C213G/C213G TF mice compared to wt mice. In hearts of male C213G/C213G TF mice, flTF mRNA was significantly increased by 9.6 times compared to hearts of wt mice suggesting a compensatory transcriptional induction of a functionally insufficient protein that may involve recently demonstrated feedback loops of the TF cytoplasmic domain[34]. In C213G/C213G TF female hearts a similar induction was seen, however with a higher variability.

Induction of TF transcription is in line with inflammatory and fibrotic remodeling seen in all hearts of both genders. To assess the protein expression and activity of C213G TF, organ lysates were prepared from heart, brain and lung. Protein expression of C213G TF was 10 times lower than expression of wtTF in brain and lung. In hearts, protein expression of C213G TF and wtTF did not differ (Figure 5B), in line with the

compensatory upregulation of gene transcription. Pro-coagulant activity was measured using a plasma clotting assay. Pro-coagulant activity of brain and lung lysates from C213G/C213G TF mice was decreased about 1000-fold compared to wt TF brains and lungs. In heart lysates, the difference in pro-coagulant activity was only about 100-fold (Figure 5C). A 10-fold reduction of protein expression in brains and lungs of C213G/C213G TF mice is in line with a 10-fold stronger decrease in pro-coagulant activity as compared to heart. In both genotypes, there was no difference between the sexes, neither in expression nor in pro-coagulant activity.

The TF allosteric disulfide is required for TF procoagulant function in macrophages

We characterized the pro-coagulant activity of the C213G TF mutant in primary bone marrow-derived macrophages. In order to assure unaltered induction of TF in IFNγ primed and 4 hour LPS stimulated macrophages [29, 30], we measured TF mRNA levels with flTF-specific primers (Figure 6A). flTF mRNA levels were significantly higher in C213G/C213G TF macrophages which is expected as in these cells both alleles of endogenous TF (yielding fully processed mRNA for flTF and asTF) were replaced with a gene that only yields the mutated flTF. Given the unimpaired mRNA induction, we next measured TF protein expression 90 minutes and 4 hours after LPS stimulation (Figure 6B). While TF induction was below the detection limit in the absence of IFNγ priming, a low molecular ~48 kDa form of TF was expressed after 90 minutes of stimulation in both IFNγ-primed wt and C213G/C213G TF macrophages. After 4 hours of stimulation, wt TF was predominantly expressed as a highly glycosylated protein which was not detected in macrophages from C213G/C213G TF mice.

Since glycosylation of TF is required for cell surface expression and procoagulant activity in intestinal epithelial cells [35], we next tested the procoagulant activity of intact macrophages. Macrophage cell surface TF is largely inactive and requires activation of the P2X7 receptor with ATP. C213G/C213G TF macrophages displayed minimal procoagulant activity on their cell surface after ATP stimulation and no TF activity or antigen was detected on EV released from these cells (Figure 6C-D). Western Blotting for other proteins typically released on ATP-induced EV[36] revealed no quantitative abnormalities in EV release from C213G/C213G TF macrophages, demonstrating that TF is selectively absent in EV derived from C213G/C213G TF macrophages (Figure 6D). In addition, measurements of prothrombinase activity showed that the release of procoagulant lipids on EV was not different between wild-type and C213G/C213G TF macrophages (Figure 6C). Thus, mutation of the allosteric disulfide of TF prevents glycosylation and normal cellular processing, leading to a severely impaired procoagulant activity in macrophages stimulated with inflammatory mediators.

Behavioral differences

Having excluded that primary differences in protein expression and activity as well as general hemostatic capacity exist between the sexes, we investigated whether behavioral differences of male and female mice may underlie differences in disease severity in homozygous C213G/C213G TF mice. At the age of 21 days, 12 homozygous C213G/C213G TF males were weaned to individual cages and housed individually up to the age of 100 days to prevent aggressive fighting. All 12 males survived to the age of 100 days, which is a significant improvement compared to group housed males ($p=0.0326$) (Figure 7A). After day 100, pulmonary hemorrhages were detected in 3 out of 12 (25%) single housed homozygous C213G/C213G TF

males (Figure 7B), in comparison to 50% lung hemorrhages in homozygous C213G/C213G TF group housed males. This experiment demonstrates that lung hemorrhages develop spontaneously in homozygous C213G/C213G TF males, but single housing reduces the risk for lung bleedings and lowers mortality.

Discussion

After the description of the importance of the TF C-terminal disulfide bridge for TF pro-coagulant activity [26] and evidence for its involvement in TF decryption [20, 21, 27] it is crucial to understand its significance in an in vivo model. In the C213G TF mouse model we observed changes similar to those previously reported in vitro: reduced protein expression, glycosylation, and surface translocation. In line with this, the pro-coagulant activity is reduced by at least a factor 100 independent of changes in protein expression. The C213G TF mutant still exhibits sufficient pro-coagulant activity to ensure embryonic development in 2/3rd of offspring and to allow early post-natal survival.

The overall phenotype of C213G/C213G TF mice shows impressive similarity to the phenotype of low-TF mice, which express a human TF transgene in the absence of mouse TF. Pro-coagulant activity in low-TF mice was estimated 1% of normal levels resulting from low expression of TF under the control of the human promoter [6]. However, low-TF mice are born in accordance with Mendelian ratios [6], while C213G TF mice displayed a reduced number of homozygous C213G/C213G TF offspring at birth. Partial developmental lethality is observed when other clotting factors (Factor V, Prothrombin) or the thrombin receptor PAR1 are knocked out [37-39]. Deficiency in PAR2, which is activated by the TF/FVIIa complex, results in a partial, but undefined developmental lethality [40], suggesting that thrombin generation and PAR1 signaling, but not PAR2 signaling, are crucial for development. Rescue experiments of murine TF (mTF) ko using different human TF transgenic lines suggested that the threshold of TF activity needed to support embryonic development is lower than that needed to maintain postpartum hemostasis, as some transgenic lines quantitatively rescue genetic deletion of mTF but rescued pups die days or weeks after birth [41]. For C213G/C213G TF embryos this either suggests that expression under the

endogenous mTF promoter may lead to different spatio-temporal expression patterns associated with different thresholds or that certain signaling functions of C213G TF are altered, whose importance for development has not been recognized yet. Given the placental hemorrhages observed in homozygous C213G/C213G TF mice, placental insufficiency might contribute to the partial developmental lethality in the latter and is in line with the low-TF phenotype exhibiting blood pooling in placentas of low-TF embryos at E14.5 [13].

Reduced survival of low-TF mice was mainly attributed to impaired left ventricular function induced by myocardial hemorrhages and fibrosis [6]. Development of cardiac fibrosis was found to be sex-dependent with lower severity in female mice and associated with downregulation of fibrinolytic urokinase plasminogen activator [42]. Although there was a sex-dependent effect on the development of cardiac fibrosis, no difference in survival was described between the sexes. No changes in heart rate, systolic, diastolic, or mean arterial blood pressure was found in C213G/C213G TF mice, suggesting that the myocardial fibrosis did not fully translate into cardiac dysfunction. At the mRNA level, cardiac TF expression was about ten times higher in C213G/C213G TF mice as compared to wt TF mice. This increase translated in a similar cardiac protein expression in C213G/C213G TF mice and wt TF mice – in contrast to lung and brain, where protein expression was lower in C213G/C213G TF mice. This observation is consistent with a compensatory elevation of transcription and may in part explain the unaltered hemodynamic parameters.

C213G/C213G TF males showed lower survival as compared to females; however, from autopsies of dead or terminally ill mice it was difficult to define the exact cause of death, particularly when all the three organs brain, heart, and lung showed hemorrhages. We therefore analyzed the incidence of sub-lethal hemorrhages in a uniform cohort of male and female C213G/C213G TF and wt TF mice, assuming that

the incidence of sub-lethal hemorrhages correlates with the incidence of terminal hemorrhages. In this healthy appearing cohort, we found a considerable degree of cardiac fibrosis in 100% of C213G/C213G TF mice, and the level of fibrosis did not differ between male and female mice. However, male C213G/C213G TF mice showed a higher incidence of lung bleedings compared to females as well as a differential pulmonary gene expression pattern. This suggests that in C213G/C213G TF mice, lung hemorrhages may represent the main reason for terminal disease. To address the question why male C213G/C213G TF mice are more prone to lung bleedings than female C213G/C213G TF mice, we investigated possible molecular differences in TF expression between the genders or functional differences in bleeding time. As neither of these parameters showed a difference between female and male homozygous C213G/C213G TF mice, we hypothesized that behavioral differences, in particular aggressive fighting, leads to aggravated pulmonary hemorrhage in homozygous C213G/C213G TF males. Inter-male aggression is a well known problem in housing of male laboratory mice, which can be modulated by genetic background as well as cage enrichment [43]. Cases of exercise induced pulmonary hemorrhage exist in healthy humans [44, 45] and spontaneous pulmonary hemorrhages are a known complication of anticoagulant therapy [46-49]. Single housing indeed reduced the incidence of pulmonary hemorrhages and significantly improved survival of homozygous C213G/C213G TF male mice with low pulmonary TF activity, suggesting that fully active TF is protective against spontaneous and exercise induced pulmonary hemorrhages. A previous report suggested that fatal lung hemorrhages may also represent a major reason for reduced survival of low-TF mice [8]. In line with this, 17% of low-TF mice die of spontaneous hemorrhages in lung, brain, and gastrointestinal tract, [7, 10].

In contrast to low-TF mice [9], we did not observe any testis calcification in C213G/C213G TF male mice. The morphology of the seminiferous tubules of the testis and the general sperm amount in the cauda epididymis seemed normal. Since the corresponding single Cys replacement in human TF is compatible with TF-FVIIa signaling[21], one possible explanation for these differences is preservation of integrin-dependent TF signaling[50] in the context of testes physiology.

In conclusion, mutation of the allosteric disulfide bond of TF leads to some reduction in protein expression and a pronounced reduction in protein activity of at least 100-fold which goes along with impaired glycosylation and cell surface expression. This impairment results in a bleeding phenotype causing partial developmental lethality and high susceptibility of lung, brain, and heart to bleedings after birth. Male mice exhibit more frequent and severe lung hemorrhages, which can be reduced by single housing preventing inter-male aggression. Thus, this study emphasizes the importance of the allosteric disulfide for proper TF expression, modification and function in vivo and the importance of functional TF for developmental and post-natal hemostasis and survival.

Funding

Funding information: GMC was supported by the German Federal Ministry of Education and Research (Infrafrontier grant 01KX1012 to MHA). WR is supported by the National Heart Lung Blood Institute (HL-60472). SHMS and FCT were supported by the Swiss Heart Foundation.

Disclosures

None.

References

1. Drake TA, Morrissey JH, Edgington TS. Selective cellular expression of tissue factor in human tissues. Implications for disorders of hemostasis and thrombosis. Am J Pathol. 1989;134(5):1087-1097.
2. Mackman N, Sawdey MS, Keeton MR, Loskutoff DJ. Murine tissue factor gene expression in vivo. Tissue and cell specificity and regulation by lipopolysaccharide. Am J Pathol. 1993;143(1):76-84.
3. Carmeliet P, Mackman N, Moons L, et al. Role of tissue factor in embryonic blood vessel development. Nature. 1996;383(6595):73-75.
4. Bugge TH, Xiao Q, Kombrinck KW, et al. Fatal embryonic bleeding events in mice lacking tissue factor, the cell-associated initiator of blood coagulation. Proc Natl Acad Sci U S A. 1996;93(13):6258-6263.
5. Toomey JR, Kratzer KE, Lasky NM, Stanton JJ, Broze GJ, Jr. Targeted disruption of the murine tissue factor gene results in embryonic lethality. Blood. 1996;88(5):1583-1587.
6. Parry GC, Erlich JH, Carmeliet P, Luther T, Mackman N. Low levels of tissue factor are compatible with development and hemostasis in mice. J Clin Invest. 1998;101(3):560-569.
7. Pawlinski R, Fernandes A, Kehrle B, et al. Tissue factor deficiency causes cardiac fibrosis and left ventricular dysfunction. Proc Natl Acad Sci U S A. 2002;99(24):15333-15338.
8. Pedersen B, Holscher T, Sato Y, Pawlinski R, Mackman N. A balance between tissue factor and tissue factor pathway inhibitor is required for embryonic development and hemostasis in adult mice. Blood. 2005;105(7):2777-2782.
9. Mackman N. Tissue-specific hemostasis in mice. Arterioscler Thromb Vasc Biol. 2005;25(11):2273-2281.

10. Bode MF, Mackman N. A combined deficiency of tissue factor and PAR-4 is associated with fatal pulmonary hemorrhage in mice. Thromb Res. 2016;146:46-50.
11. Bastarache JA, Sebag SC, Clune JK, et al. Low levels of tissue factor lead to alveolar haemorrhage, potentiating murine acute lung injury and oxidative stress. Thorax. 2012;67(12):1032-1039.
12. Antoniak S, Tatsumi K, Hisada Y, et al. Tissue factor deficiency increases alveolar hemorrhage and death in influenza A virus-infected mice. J Thromb Haemost. 2016;14(6):1238-1248.
13. Erlich J, Parry GC, Fearns C, et al. Tissue factor is required for uterine hemostasis and maintenance of the placental labyrinth during gestation. Proc Natl Acad Sci U S A. 1999;96(14):8138-8143.
14. Pawlinski R, Pedersen B, Erlich J, Mackman N. Role of tissue factor in haemostasis, thrombosis, angiogenesis and inflammation: lessons from low tissue factor mice. Thromb Haemost. 2004;92(3):444-450.
15. Osterud B. Tissue factor expression in blood cells. Thromb Res. 2010;125 Suppl 1:S31-34.
16. Swystun LL, Liaw PC. The role of leukocytes in thrombosis. Blood. 2016;128(6):753-762.
17. Bach RR. Tissue factor encryption. Arterioscler Thromb Vasc Biol. 2006;26(3):456-461.
18. Pendurthi UR, Ghosh S, Mandal SK, Rao LV. Tissue factor activation: is disulfide bond switching a regulatory mechanism? Blood. 2007;110(12):3900-3908.
19. Kothari H, Nayak RC, Rao LV, Pendurthi UR. Cystine 186-cystine 209 disulfide bond is not essential for the procoagulant activity of tissue factor or for its de-encryption. Blood. 2010;115(21):4273-4283.

20. Chen VM, Ahamed J, Versteeg HH, Berndt MC, Ruf W, Hogg PJ. Evidence for activation of tissue factor by an allosteric disulfide bond. Biochemistry. 2006;45(39):12020-12028.
21. Ahamed J, Versteeg HH, Kerver M, et al. Disulfide isomerization switches tissue factor from coagulation to cell signaling. Proc Natl Acad Sci U S A. 2006;103(38):13932-13937.
22. Reinhardt C, von Bruhl ML, Manukyan D, et al. Protein disulfide isomerase acts as an injury response signal that enhances fibrin generation via tissue factor activation. J Clin Invest. 2008;118(3):1110-1122.
23. Langer F, Spath B, Fischer C, et al. Rapid activation of monocyte tissue factor by antithymocyte globulin is dependent on complement and protein disulfide isomerase. Blood. 2013;121(12):2324-2335.
24. Subramaniam S, Jurk K, Hobohm L, et al. Distinct contributions of complement factors to platelet activation and fibrin formation in venous thrombus development. Blood. 2017;129(16):2291-2302.
25. Muller-Calleja N, Ritter S, Hollerbach A, Falter T, Lackner KJ, Ruf W. Complement C5 but not C3 is expendable for tissue factor activation by cofactor-independent antiphospholipid antibodies. Blood Adv. 2018;2(9):979-986.
26. Rehemtulla A, Ruf W, Edgington TS. The integrity of the cysteine 186-cysteine 209 bond of the second disulfide loop of tissue factor is required for binding of factor VII. J Biol Chem. 1991;266(16):10294-10299.
27. van den Hengel LG, Osanto S, Reitsma PH, Versteeg HH. Murine tissue factor coagulant activity is critically dependent on the presence of an intact allosteric disulfide. Haematologica. 2013;98(1):153-158.
28. van den Hengel LG, van den Berg YW, Reitsma PH, Bos MH, Versteeg HH. Evolutionary conservation of the tissue factor disulfide bonds and identification of

a possible oxidoreductase binding motif. J Thromb Haemost. 2012;10(1):161-162.

29. Furlan-Freguia C, Marchese P, Gruber A, Ruggeri ZM, Ruf W. P2X7 receptor signaling contributes to tissue factor-dependent thrombosis in mice. J Clin Invest. 2011;121(7):2932-2944.
30. Rothmeier AS, Marchese P, Petrich BG, et al. Caspase-1-mediated pathway promotes generation of thromboinflammatory microparticles. J Clin Invest. 2015;125(4):1471-1484.
31. Mu J, Adamson SL. Developmental changes in hemodynamics of uterine artery, utero- and umbilicoplacental, and vitelline circulations in mouse throughout gestation. Am J Physiol Heart Circ Physiol. 2006;291(3):H1421-1428.
32. Pequignot MO, Provost AC, Salle S, et al. The retinal pigment epithelium undergoes massive apoptosis during early differentiation and pigmentation of the optic cup. Mol Vis. 2011;17:989-996.
33. Hydrocephalus in Laboratory Mice. 2003 [cited 25.09.2012]; Issue 490, Summer:[Available from: http://jaxmice.jax.org/jaxnotes/archive/490f.html
34. Kurakula K, Koenis DS, Herzik MA, Jr., et al. Structural and cellular mechanisms of peptidyl-prolyl isomerase Pin1-mediated enhancement of Tissue Factor gene expression, protein half-life, and pro-coagulant activity. Haematologica. 2018;103(6):1073-1082.
35. Reinhardt C, Bergentall M, Greiner TU, et al. Tissue factor and PAR1 promote microbiota-induced intestinal vascular remodelling. Nature. 2012;483(7391):627-631.
36. Rothmeier AS, Marchese P, Langer F, et al. Tissue Factor Prothrombotic Activity Is Regulated by Integrin-arf6 Trafficking. Arterioscler Thromb Vasc Biol. 2017;37(7):1323-1331.

37. Connolly AJ, Ishihara H, Kahn ML, Farese RV, Jr., Coughlin SR. Role of the thrombin receptor in development and evidence for a second receptor. Nature. 1996;381(6582):516-519.
38. Cui J, O'Shea KS, Purkayastha A, Saunders TL, Ginsburg D. Fatal haemorrhage and incomplete block to embryogenesis in mice lacking coagulation factor V. Nature. 1996;384(6604):66-68.
39. Sun WY, Witte DP, Degen JL, et al. Prothrombin deficiency results in embryonic and neonatal lethality in mice. Proc Natl Acad Sci U S A. 1998;95(13):7597-7602.
40. Damiano BP, Cheung WM, Santulli RJ, et al. Cardiovascular responses mediated by protease-activated receptor-2 (PAR-2) and thrombin receptor (PAR-1) are distinguished in mice deficient in PAR-2 or PAR-1. J Pharmacol Exp Ther. 1999;288(2):671-678.
41. Parry GC, Mackman N. Mouse embryogenesis requires the tissue factor extracellular domain but not the cytoplasmic domain. J Clin Invest. 2000;105(11):1547-1554.
42. Davis DR, Wilson K, Sam MJ, et al. The development of cardiac fibrosis in low tissue factor mice is gender-dependent and is associated with differential regulation of urokinase plasminogen activator. J Mol Cell Cardiol. 2007;42(3):559-571.
43. Van Loo PL, Van Zutphen LF, Baumans V. Male management: Coping with aggression problems in male laboratory mice. Lab Anim. 2003;37(4):300-313.
44. Ghio AJ, Ghio C, Bassett M. Exercise-induced pulmonary hemorrhage after running a marathon. Lung. 2006;184(6):331-333.
45. Ko YC, Dai MP, Ou CC. Playing saxophone induced diffuse alveolar hemorrhage: a case report. Ir J Med Sci. 2010;179(1):137-139.

46. Santalo M, Domingo P, Fontcuberta J, Franco M, Nolla J. Diffuse pulmonary hemorrhage associated with anticoagulant therapy. Eur J Respir Dis. 1986;69(2):114-119.
47. Kok LC, Sugihara J, Druger G. First case report of spontaneous pulmonary hemorrhage following heparin therapy in acute myocardial infarction. Hawaii Med J. 1996;55(5):83-84.
48. Sitges M, Villa FP. Massive pulmonary hemorrhage in a patient treated with a platelet glycoprotein IIb/IIIa inhibitor. Int J Cardiol. 1997;62(3):269-271.
49. Finley TN, Aronow A, Cosentino AM, Golde DW. Occult pulmonary hemorrhage in anticoagulated patients. Am Rev Respir Dis. 1975;112(1):23-29.
50. Rothmeier AS, Liu E, Chakrabarty S, et al. Identification of the integrin-binding site on coagulation factor VIIa required for proangiogenic PAR2 signaling. Blood. 2018;131(6):674-685.

Figure legends

Figure 1: **Genetic targeting, genotype distributions and survival.** (A) The murine TF allele was targeted with a replacement-type vector containing the murine flTF coding sequence with T721G nucleotide exchange in exon 5, flanked by 3 kb 5' and 5.2 kb 3' homology arms. Diphtheria toxin (dt) was used for negative selection. After homologous recombination into 129P2/OlaHsd embryonic stem cells, a loxP flanked neomycin resistance cassette was removed by transfection with a Cre expression plasmid. (B) Genotype distribution of offspring from heterozygous breeding pairs on a B6 background were analyzed at different time points. Genotype distributions were compared to a mendelian 25%/50%/25% distribution as well as to the distributions at other time points. (C) Reduced survival of homozygous C213G TF mice. Survival curve of homozygous male and female C213G/C213G TF offspring on mixed and B6 genetic background (male mixed n=32, female mixed n=32, male B6 n=32, female B6 n=43). Dead and diseased mice meeting the termination criteria were both included in the analysis.

Figure 2: Figure 2: **Macroscopic images of lung hemorrhages and iron detection (Prussian Blue staining) in heart, lung and brain hemorrhages.** (A) Representative macroscopic images of lung bleedings in male and female homozygous C213G/C213G TF mice. (B) Lung, (C) heart, and (D) brain consecutive sections from wt and homozygous C213G/C213G TF mice were stained with hematoxylin and eosin (H&E) for morphological analysis and Prussian Blue to show ferric iron (Fe^{3+}) in blood. The area of the higher magnification pictures (20x) is demarcated with a rectangle in the lower magnification ones (aprox. 1.45x in heart/brain and 5x in lung). Iron deposits within lung macrophages are particularly obvious in B.

Figure 3: **Histological images of myocarditis and myocardial fibrosis, gene profile in heart and lung tissue.** (A) Heart sections of wt and homozygous C213G/C213G TF mice were stained with hematoxylin and eosin (H&E). Immune infiltrates are visible in the myocardium of C213G/C213G TF animals. The area of the higher magnification picture (40x) is shown with a rectangle in the lower magnification one (15x). (B) Consecutive sections from wt and homozygous C213G/C213G TF mice were stained with hematoxylin and eosin (H&E) for morphological analysis and Picro-sirius Red for better visualization of collagen. The area of the higher magnification (20x) pictures is demarcated with a rectangle in the lower magnification ones (aprox. 1.45x). (C) Heatmaps of significantly (FDR<10%) regulated genes between homozygous C213G/C213G TF and wt mice in heart and lung tissues. Genes are shown, if they are regulated in either male or female animals per tissue. Yellow (blue) indicates down (up) regulation compared to the mean expression of wt mice.

Figure 4: **Bleeding time and blood counts.** (A) Bleeding times after amputation of 5 mm tail tip; male wt n=19, female wt n=13, male C213G/C213G n=15, female C213G/C213G n=11; **p<0.01, ***p<0.001. (B) Blood count analysis in C213G/C213G TF and wt mice in with Sysmex XT-2000iV. Some of the values where significantly different between C213G/C213G TF mice and wt TF mice. However, absolute differences were all minor.

Figure 5: **TF expression and activity in brain, lung and heart.** (A) Semi-quantitative RT-PCR in brain, lung, and heart of male and female homozygous

C213G/C213G TF mice and wt TF mice using flTF-specific primers and normalization for β-actin (n=6, *p<0.05). (B) Representative blots and quantification of TF protein expression in brain, lung and heart of male and female homozygous C213G/C213G TF mice and wt TF mice (n=4, **p<0.01, ***p<0.001). (C) Plasma clotting time measurements of TF activity in brain, lung and heart of male and female homozygous C213G/C213G TF and wt TF mice (n=4, **p<0.01, ***p<0.001).

Figure 6: **TF expression and EV release in bone marrow-derived macrophages.** (A) TF mRNA levels were determined by semi-quantitative RT-PCR using flTF-specific primers and normalization for β-actin. Bone marrow-derived macrophages cultured overnight without or with IFNγ (100 ng/ml) were stimulated with 1 mg/ml LPS for 4 hours; wt n=5, C213G/C213G n=4; ***p<0.001. (B) Western-blotting for TF with a polyclonal anti-mouse TF antibody of membrane fractions from macrophages with or without overnight IFNγ priming stimulated with 1 mg/ml LPS for the indicated times (representing two independent experiments). (C) TF cellular and EV activity measured by FXa generation assay of INFv primed and LPS stimulated macrophages with or without activation of the P2X7 receptor with 5 mM ATP for 30'; n=3, **p<0.05, **p<0.01*. Prothrombinase activity of the same EV preparations was determined as a measure for the release of procoagulant, PS-expressing MP. (D) Protein composition of EV released after ATP stimulation for 30' was evaluated by Western-blotting for TF, integrin b1, and b-actin. Densitometric quantification of protein levels from 3 independent experiments showed that levels on EV from C213G/C213G TF macrophages were 1.4 ± 1.1 for integrin b1 and 1.4 ± 1.7 for b-actin relative to wt-derived EV levels (representing two independent experiments).

Figure 7: **Single housing reduces incidence of lung bleedings and lethality in homozygous C213G/C213G male mice.** (A) All 12 single housed C213G/C213G TF males survived up to 100 days, in contrast to C213G/C213G TF males, which were group housed (n=32). (B) Incidence of lung bleedings was reduced from 50% to 25% in homozygous C213G/C213G TF males.

Figure 1

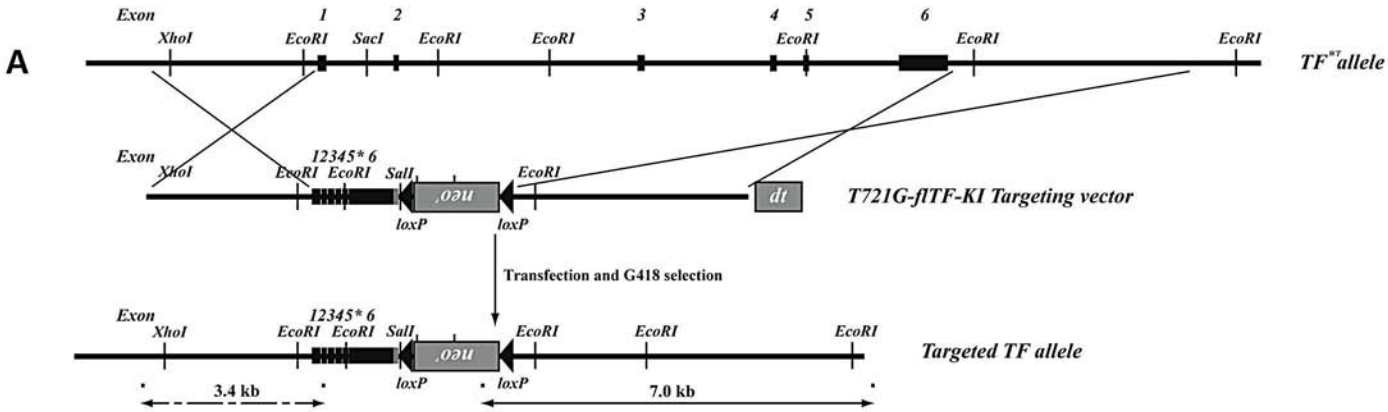

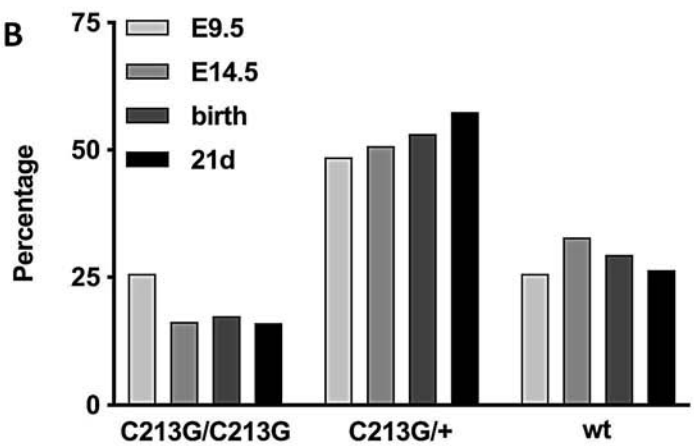

	C213G/ C213G	C213G/+	wt	n
E9.5	25.7%	48.6%	25.7%	70
E14.5	16.4%	50.8%	32.8%	67
birth	17.5%	53.1%	29.4%	320
d21	16.1%	57.5%	26.4%	889

X^2-test	E14.5	birth	21d	mendel
E9.5	0.3642	0.2808	0.0963	0.9718
E14.5	-	0.8521	0.5379	0.163
birth		-	0.4607	0.0058
21d			-	0

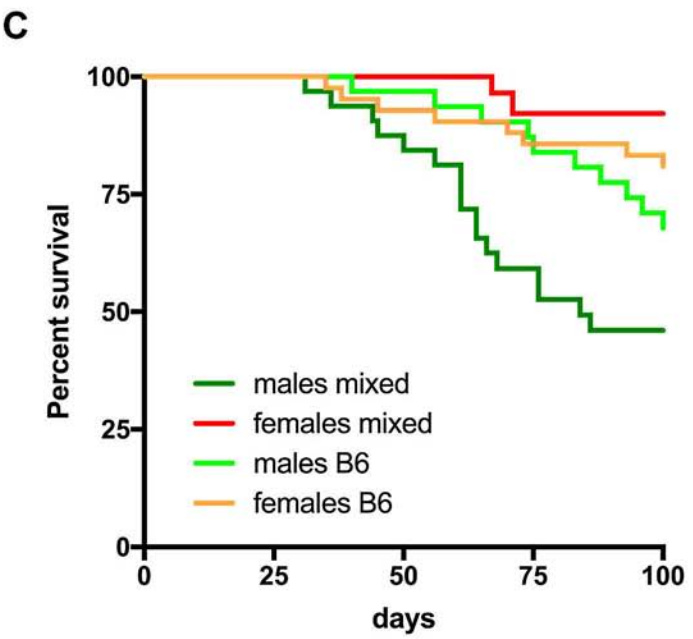

Figure 2

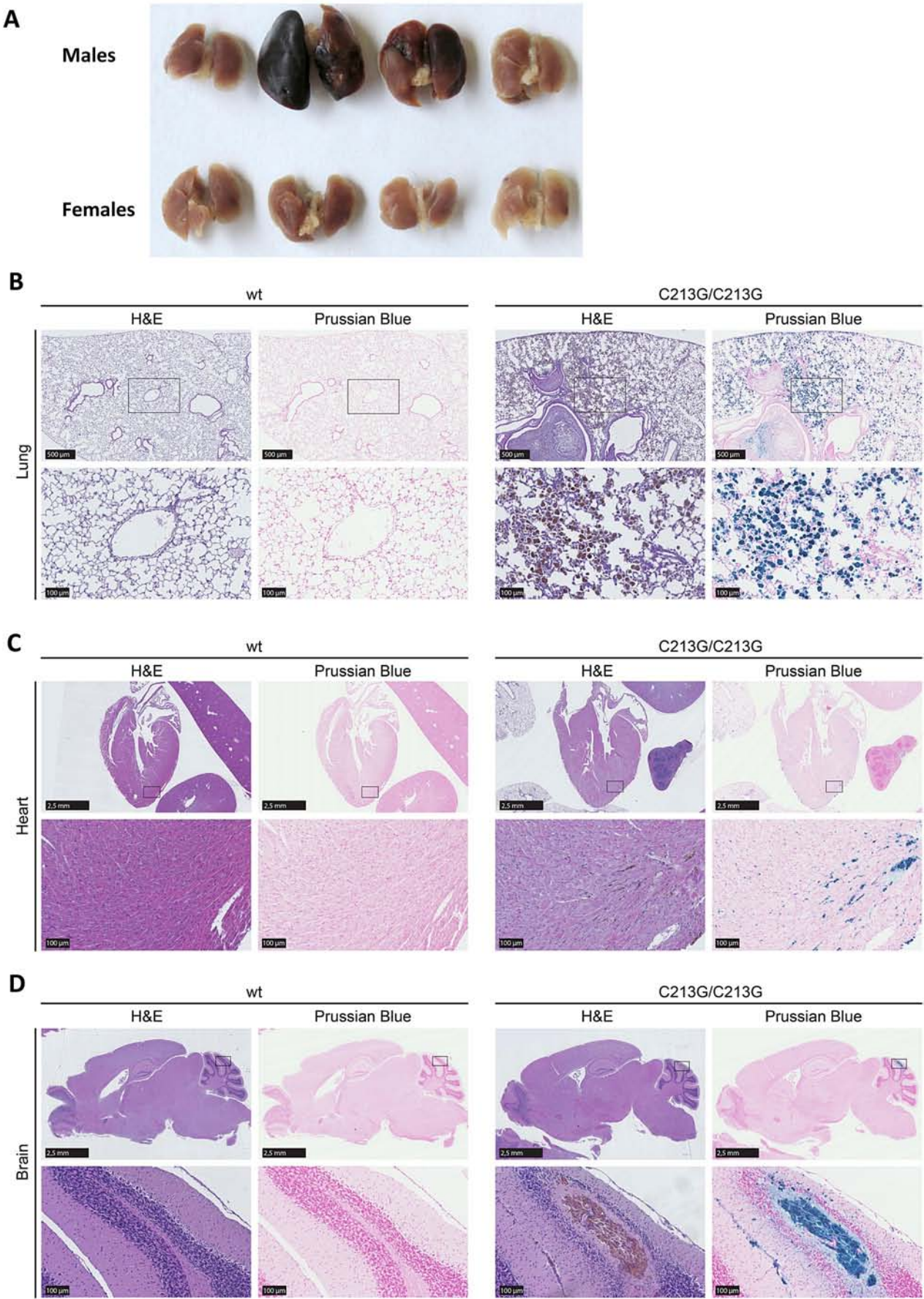
A
Males
Females
B
wt
C213G/C213G
H&E
Prussian Blue
Lung
500 µm
100 µm
C
Heart
2.5 mm
D
Brain

Figure 3

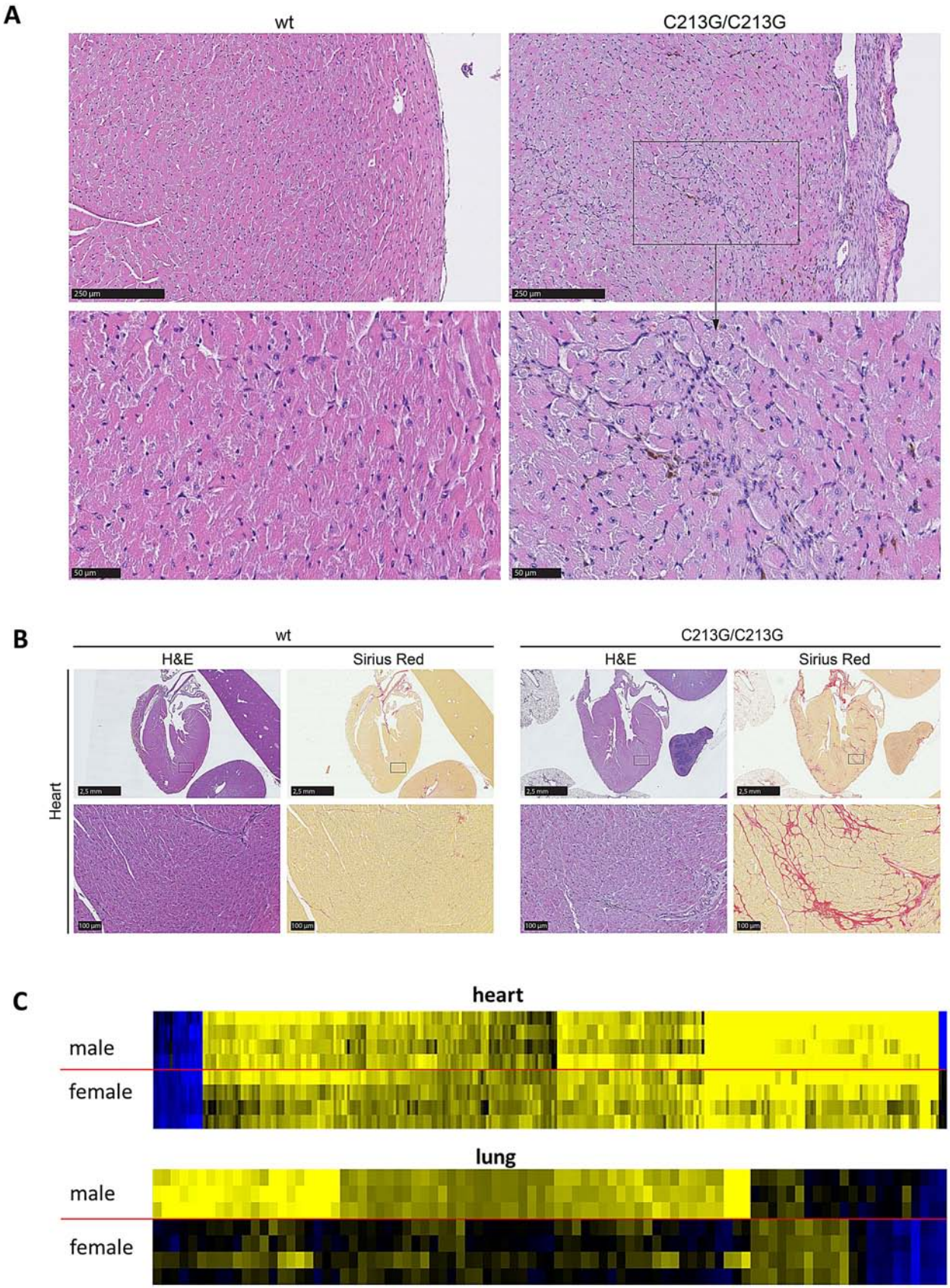
A
wt
C213G/C213G
250 µm
250 µm
50 µm
50 µm
B
wt
C213G/C213G
H&E
Sirius Red
H&E
Sirius Red
Heart
2.5 mm
2.5 mm
2.5 mm
2.5 mm
100 µm
100 µm
100 µm
100 µm
C
heart
male
female
lung
male
female

Figure 4

A

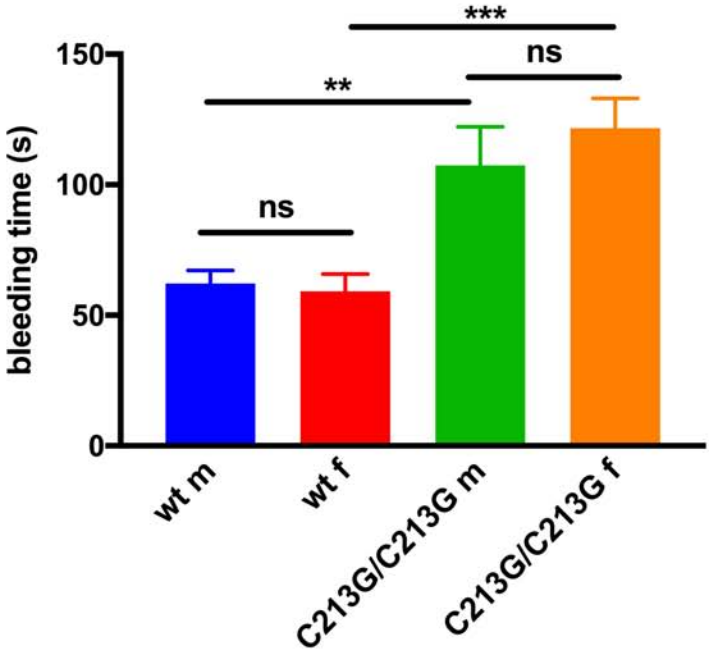

B

Group: fITF (6 month) additional group	Control (A)		Mutant (B)	
Sex	**Male**	**Female**	**Male**	**Female**
Number of animals tested	11	10	8	7
WBC [10^3/µl]	9.2 ± 0.62	5.9 ± 0.47	9.1 ± 0.49	6.5 ± 0.84
RBC [Mio/µl]	9.7 ± 0.2	10.1 ± 0.11	10.1 ± 0.22	9.9 ± 0.17
PLT [10^3/µl]	1942 ± 70	1453 ± 27.9	1860 ± 111.4	1640 ± 59.7
Hemoglobin [g/dl]	14 ± 0.22	14.7 ± 0.15	14.1 ± 0.21	14.1 ± 0.22
Hematocrit [%]	47 ± 0.91	48.8 ± 0.5	48.7 ± 0.71	47.5 ± 0.65
MCV [fl]	48.3 ± 0.35	48.4 ± 0.1	48.3 ± 0.57	48 ± 0.22
MCH [pg]	14.4 ± 0.11	14.6 ± 0.06	14 ± 0.19	14.3 ± 0.11
MCHC [g/dl]	29.9 ± 0.25	30.1 ± 0.14	29 ± 0.14	29.7 ± 0.17
RDW-CV [%]	22.1 ± 0.52	21.6 ± 0.19	22.8 ± 0.44	21.7 ± 0.21
MPV [fl]	6.58 ± 0.03	6.66 ± 0.07	6.79 ± 0.08	6.77 ± 0.09
PDW [fl]	7.11 ± 0.05	7.2 ± 0.09	7.39 ± 0.11	7.23 ± 0.12
P-LCR [%] (PV>12fl)	4.28 ± 0.15	4.81 ± 0.34	5.31 ± 0.37	5.21 ± 0.45
Ret [Mio/µl]	0.43 ± 0.02	0.44 ± 0.03	0.48 ± 0.03	0.56 ± 0.06
Ret [%]	4.38 ± 0.17	4.4 ± 0.22	4.75 ± 0.31	5.69 ± 0.64
LF Ret [%]	42.65 ± 0.96	43.63 ± 0.62	41.4 ± 0.99	41.27 ± 0.83
MF Ret [%]	17.29 ± 0.42	18.38 ± 0.51	18.66 ± 0.23	19.14 ± 0.52
HF Ret [%]	40.06 ± 1.04	37.99 ± 0.85	39.94 ± 1	39.59 ± 0.79
Immature Ret [%]	57.35 ± 0.96	56.37 ± 0.62	58.6 ± 0.99	58.73 ± 0.83

Figure 5

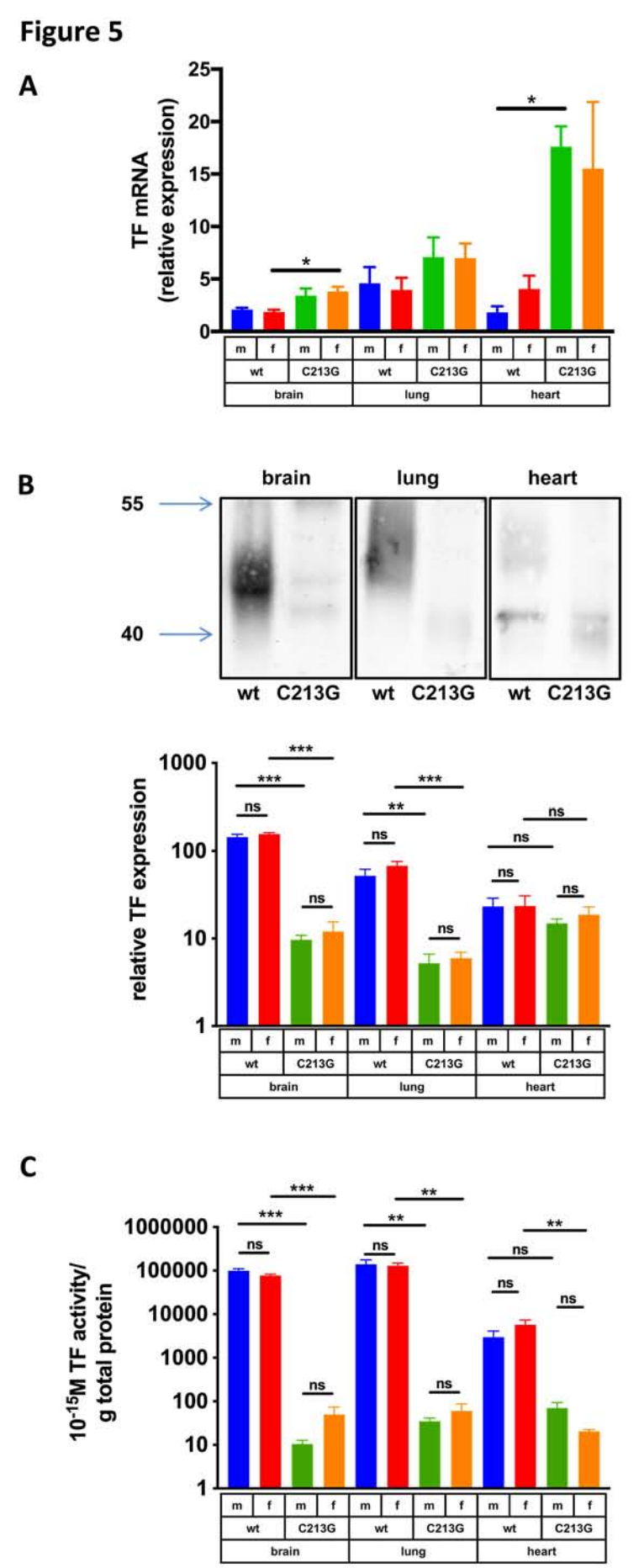
A
TF mRNA (relative expression)
25
20
15
10
5
0
*
*
m f m f m f m f m f m f
wt C213G wt C213G wt C213G
brain lung heart
B
brain lung heart
55
40
wt C213G wt C213G wt C213G
relative TF expression
1000
100
10
1
***
***
ns
***
**
ns
ns
ns
ns
ns
ns
ns
ns
ns
m f m f m f m f m f m f
wt C213G wt C213G wt C213G
brain lung heart
C
10-15M TF activity/ g total protein
1000000
100000
10000
1000
100
10
1
***
***
ns
**
**
ns
ns
ns
ns
ns
ns
ns
m f m f m f m f m f m f
wt C213G wt C213G wt C213G
brain lung heart

Figure 6

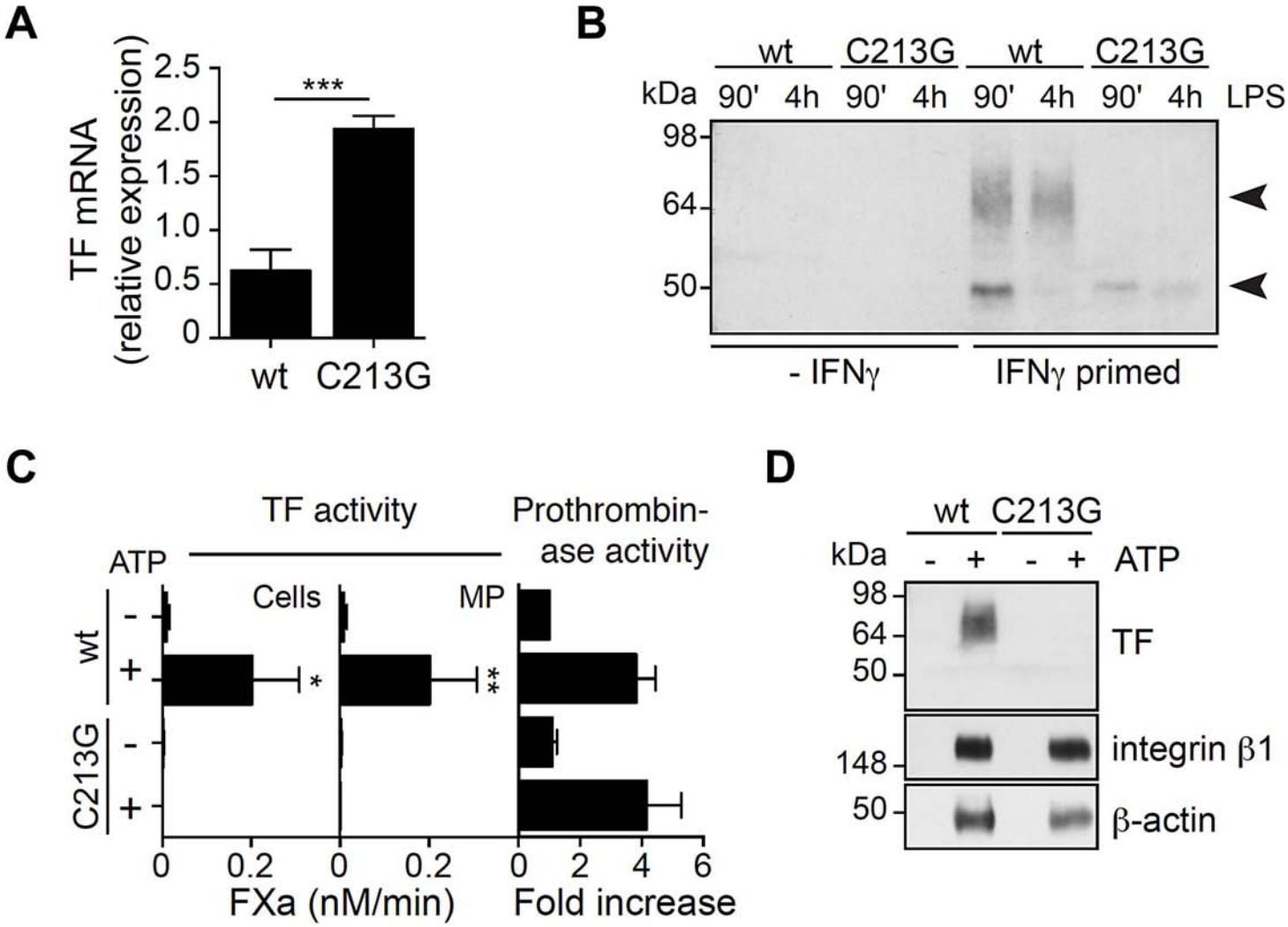
A
TF mRNA (relative expression)
2.5
2.0
1.5
1.0
0.5
0
***
wt
C213G
B
wt
C213G
wt
C213G
kDa
90'
4h
90'
4h
90'
4h
90'
4h
LPS
98
64
50
- IFNγ
IFNγ primed
C
TF activity
Prothrombin-ase activity
ATP
Cells
MP
wt
C213G
-
+
-
+
*
**
0
0.2
0
0.2
0
2
4
6
FXa (nM/min)
Fold increase
D
wt
C213G
kDa
-
+
-
+
ATP
98
64
50
TF
148
50
integrin β1
β-actin

Figure 7

A

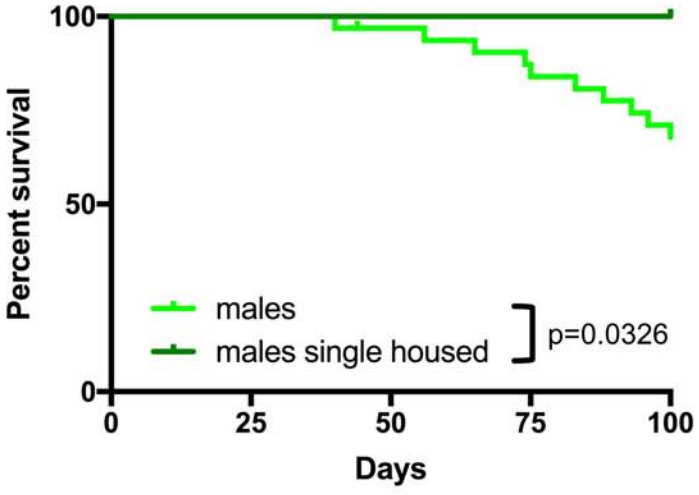
100
50
0
Percent survival
males
males single housed
p=0.0326
0
25
50
75
100
Days

B

Supplemental material: Methods

Construction of the C213G TF targeting vector

The vector generated for murine TF (mTF) targeting is a replacement-type vector containing two long arms of homology. The coding sequence of the murine full length TF isoform containing a T721G mutation in its open reading frame was inserted into KpnI/NotI restriction sites of a LNTK vector (PolyGene AG, Ruemlang, Switzerland) located 5' to a neomycin resistance gene, flanked by two loxP sites (floxed neo). A 3 kb genomic sequence 5' upstream of the first exon of the TF gene, and a 5.2 kb Bsp120I/NotI restriction fragment located 3' downstream of the last exon of the TF gene, were used as the left and the right arms of homology, respectively. A diphtheria toxin alpha chain minigene (dtα) under the control of the DNA polymerase II promoter served as a negative selection marker; dtα was inserted into the targeting vector on its 3'-end as a 1.2 kb Bsp120I/NotI restriction fragment. The targeting vector was linearized on the NotI restriction site located on its 3'-end prior to electroporation. Embryonic stem cell transfection (129P2/OlaHsd), screening, neomycin excision as well as blastocyst injection was conducted by PolyGene AG (Ruemlang, Switzerland). Chimeric mice were bred with C57BL/6J mice.

Animals

One mouse colony was maintained by breeding of heterozygous animals on a mixed 129P2/OlaHsd-C57BL/6J background with a mean of 50% from each background strain. In parallel, mice were backcrossed to C57BL/6J (B6) by a speed congenic approach: from each generation the two offspring with the highest percentage of B6 background was chosen for further backcrossing. The genetic background was analyzed screening 96 polymorphic microsatellite markers (Elchrom Scientific AG,

Cham, Switzerland). After 5 backcrosses 3 mice had reached 100% B6 background and founded a B6 colony, which was maintained by breeding of heterozygous animals. After the discovery of a strain phenotype with increased lethality, the animals were checked daily and euthanized, when they developed pronounced affliction (apathy, dyspnea, neurological symptoms). Dead and euthanized strained animals were both included in the survival analysis with their age at death or euthanasia. Two cohorts of mice derived from the B6-colony were used for systemic phenotyping including hematological analyses and blood pressure measurement. Mice were maintained in individually ventilated cages with water and standard mouse chow (Altromin no. 1314) according to the institutional housing conditions and local laws. All tests performed were approved by the responsible authority of the local government.

Embryonic analysis

For embryonic analyses heterozygous C213G/+ TF mice were bred and females were controlled for plugs every morning. The day of the plug was considered to be E0.5.

At E9.5, uteri were fixed with 4% formalin in PBS for at least 4 days. Using a razor blade, individual implantation sites were separated and each implantation site was halved transversely to the uterus. A piece of embryonic or yolk sac tissue was taken from one half and washed with PBS before genotyping, the other half was put back to 4% formalin in PBS. After genotyping, the remaining half was embedded to paraffin and sectioned to do immunohistochemical staining of smooth muscle α-actin (Sigma, F3777).

At E14.5 uteri were dissected, a piece of yolk sac was taken from every implantation site for genotyping, while fetus and placenta were fixed in 4% formalin in PBS.

Pathological analysis

C213G/C213G TF (11 female and 10 male) and control (5 female and 5 male) mice were sacrificed according to approved protocols and all organs were examined macroscopically during necropsy. For microscopical analysis, 30 organs (see www.mouseclinic.de for more info) were immersion-fixed in 4% neutral buffered formalin and subsequently embedded in paraffin. Four-micrometer thick sections were either stained with hematoxylin and eosin (H&E) for general histological analysis, Picro-sirius Red for better visualization of collagen or Prussian Blue for iron deposits. Finally, slides were scanned using a Hamamatsu NanoZoomer 2.0HT digital scanner and analysed with NDP.view2 software (Hamamatsu Photonics, Japan).

Expression profiling

Total RNA was isolated from organs just before microarray hybridization. Organs (heart, lung and brain) were thawed in Trizol Reagent (Sigma), homogenized using a Polytron homogenizer (Heidolph) and total RNA was extracted from individual samples using RNeasy Midi kits (Qiagen) following the manufacturer's protocol. 2 µg RNA aliquots were run on a formaldehyde agarose gel to check for RNA integrity and concentrations were calculated from OD260/280 measurement. The RNA was stored at -80°C in RNase free water (Qiagen).

Four biological replicates for each genotype group were performed (four mutants and four controls). Therefore, 500 ng of total RNA was amplified and biotinylated in a single round using the Illumina TotalPrep RNA Amplification Kit (Ambion). 750 ng of albelled and amplified RNA was hybridized on Illumina MouseRef8 v2.0 Expression

Bead Chips containing about 25K probes. Staining and scanning (Illumina HiScan Array Reader) was done according to the Illumina expression protocol.

Bleeding time

After onset of anesthesia, tails were prewarmed in a 37°C water bath for 10 min. Then 0.5 mm of the tail tip was amputated and the tail was immediately put back to 37°C PBS. The time to cessation of bleeding was measured.

Blood Withdrawal and Storage

Blood samples were collected from isoflurane-anesthetized mice from the retro-bulbar sinus with non-heparinized glass capillaries (1.0 mm in diameter; Neo-lab; Munich, Germany). A proportion of 50µl was collected in an EDTA-coated end-to-end capillary and diluted 1:5 with CellPack buffer in prefilled capillary tubes (Sysmex, Art.No 99940020) and mixed thoroughly for hematological measurements. Samples were placed on a rotary agitator at room temperature for until analysis.

Hematology

Diluted samples were used to determine complete blood cell counts using a Sysmex XT2000iV device (Sysmex Deutschland GmbH, Norderstedt, Germany) by applying the capillary mode according to the instructions of the manufacturer as described previously[1]

Tail-cuff blood pressure measurement

Blood pressure was measured in non-anesthetized mice with a non-invasive tail-cuff method using the MC4000 Blood Pressure Analysis Systems (Hatteras Instruments Inc., Cary, North Carolina, USA). Four animals were restrained on a pre-warmed

metal platform in metal boxes. The tails were looped through a tail-cuff and fixed in a notch containing an optical path with a LED light and a photosensor. The blood pulse wave in the tail artery is detected as transformed into an optical pulse signal by measurement of light extinction. Pulse detection, cuff inflation and pressure evaluation are automated by the system software. After five initial inflation runs for habituation, 12 measurement runs are performed for each animal in one session. Runs with movement artifacts are excluded. After one day of training, in which the animals are habituated to the apparatus and protocol, the measurements are performed on four consecutive days between 8:30 and 11:30 AM.

TF expression analysis

RNA was extracted from heart, lung or brain using TRIzol Reagent (Molecular Research Center), according to the manufacturer's protocol. Five µg of total RNA were used to synthesize cDNA using reverse transcriptase (Stratagene, La Jolla, CA) and random hexamer primers. Transcript levels were quantified by Real Time PCR using SyBr Green Master Mix (Applied Biosystems) on an Applied Biosystems 7300 System using primers specific for flTF: 5' TCAAGCACGGGAAAGAAAAC (TF forward) and 5' CTGCTTCCTGGGCTATTTTG (TF reverse) and normalized for β-actin levels. Relative expression levels represent multiples of ten of $2^{(Ct[flTF]-Ct[\beta\text{-actin}])}$. Protein was extracted by manual grinding of organ tissue in lysis buffer containing 50 mM octylglucoside, 50 mM Tris, 150 NaCl, 10 µg/µl aprotinin and 10 µg/µl leupeptin pH 7.4. Lysates were precipitated with -20°C aceton overnight and resuspended in non-reducing sample buffer with careful sonication. Samples were separated by 10% SDS-PAGE and transferred to a PVDF membrane (Immobilion®-FL, Millipore). The membrane was stained with anti-mouse TF rabbit antiserum (R8084) [2] and anti-human GAPDH (cross-reactive to mouse) mouse monoclonal (MAB374, Millipore)

primary antibodies, followed by staining with goat anti-rabbit 800CW and donkey anti-mouse 680 LT (both LI-COR® Biosciences) secondary antibodies. Staining was visualized on an Odyssey imager and quantified using the corresponding application software (version 3.0; both LI-COR® Biosciences)

TF activity

At E9.5 uteri were dissected. Tissues were snap-frozen and yolk sacs were used for genotyping. Tissues were lysed in HEPES-saline containing 0.02% sodium azide (HBS) and diluted in HBS containing 1mg/ml BSA and 50 µM phospholipid vesicles (70% phosphatidylcholine (PC) and 30% phosphatidylserine (PS), Avanti polar lipids) to measure TF activity using a plasma clotting assay. Human and mouse citrated plasma was mixed 9:1 (50µl) and prewarmed together with the sample (50µl) or a reference (recombinant lipidated human TF, American Diagnostica). After addition of 25 mM $CaCl_2$ (50µl) clotting times were measured. Clotting times were normalized to a standard curve and the total protein concentration of the sample.

Color coded gene regulation profiles

Illumina Genomestudio 2011.1 software was used for background correction and normalization of the data (quantile algorithm). The remaining negative expression values were corrected by introducing an offset. The identification of significant gene regulation was performed using SAM (Significant Analysis of Microarrays) included in the TM4 software package. Genes were ranked according to their relative difference value d(i), a score assigned to each gene on the basis of changes in gene expression levels relative to the standard deviation. Genes with d(i) values greater than a threshold were selected as significantly differentially expressed in a one class analysis. The percentage of such genes identified by chance is the false discovery

rate (FDR). To estimate the FDR, nonsense genes were identified by calculation 1000 permutations of the measurements. The selection of the top differentially expressed genes with reproducible up- or down-regulation includes less than 10% false positives (FDR) in combination with fold change > 1.5.
Functional enrichment analyses were generated through the use of QIAGEN's Ingenuity Pathway Analysis (IPA®, QIAGEN Redwood City, www.qiagen.com/ingenuity) and using GePS software (Genomatix, Germany)

Macrophage experiments

Isolation and freezing of bone marrow cells: Femura and tibiae were dissected and cleaned from soft tissue. After removing the epiphyses, bones were flushed with RPMI. Bone marrow was suspended by pipetting and cells were counted. After centrifugation at 200 g, cells were resuspended in 90% FCS, 10% DMSO and slowly frozen to -80 and then liquid nitrogen on the next day.
Bone marrow-derived macrophages (BMDM): BMDM were generated from total bone marrow cells cultured for 7 days in DMEM, 10% FCS, 20% L cell medium, 1 mM L-Glutamine, penicillin/streptomycin as described previously[3]. Cells were plated at 1 x 10^6 cells/well in a 12-well plate and cultured overnight in the presence of 100 ng/ml IFNγ (Peprotech). Macrophages were typically stimulated with 1 µg/ml LPS (S.abortus equi, Enzo Life Sciences) for 4 hours prior to functional characterization. Cells were rinsed once and stimulated in BSS buffer (0.13 M Na-gluconate, 0.02 M HEPES, 5 mM glucose, 5 mM glycine, 5 mM KCl, 1 mM MgCl2, pH 7.5) with 5 mM ATP (Roche) for 30'. Cell supernatants were cleared from debris in an Eppendorf centrifuge at 1000 rpm at 4ºC for 10' and MP were recovered by centrifugation at 16,000 g at 4ºC for 1 hour. Pellets were resuspended in 150 µl HBS (10 mM Hepes,

pH 7.4, 137 mM NaCl, 5.3 mM KCl, 1.5 mM CaCl2) for FXa generation or prothrombinase assays and in SDS-sample buffer for Western Blotting.

Functional assays: Cell surface TF activity was determined with 0.5 nM FVIIa (kindly provided by L. Petersen, Novo Nordisk) and 50 nM FX (Haematologic Technologies) in HBS by measuring a time course of FXa generation. TF MP activity was measured in HBS with 2 nM VIIa and 100 nM FX by determining a time course of FXa generation that was quantified after quenching in EDTA with the chromogenic substrate (Spectrozyme FXa, American Diagnostica). MP prothrombinase activity was measured in HBS with 10 nM FVa, 5 nM FXa and 500 nM prothrombin (Haematologic Technologies) at ambient temperature, and quantification of thrombin generation with the chromogenic substrate Spectrozyme TH (American Diagnostica).

Western blotting: We used the following antibodies for detection of proteins associated with MP by Western blotting: polyclonal rabbit anti-mouse TF (R8084) and polyclonal anti-integrin β1 [2], and anti-β-actin (Sigma-Aldrich). For detection of cell-associated TF, we prepared membrane fractions from cells using repeated Triton-X114 phase separation of cell lysed with 1% Triton-X114 (0.1 M Tris pH 8.5, 10 mM EDTA, 1 mM PMSF) and solubilized the acetone washed detergent pellets in SDS-sample buffer (Invitrogen).

RNA extraction and qPCR: RNA was isolated from macrophages using TRIzol Reagent (Life Technologies) and 1 µg RNA was transcribed into cDNA with SuperScript III First-Strand Synthesis System (Invitrogen). Transcript levels were quantified by Real Time PCR using SyBr Green Master Mix (Applied Biosystems) on an Applied Biosystems 7300 System and normalized for β-actin levels. We used an intron-spanning primer pair that was anchored in Exon 5 and only amplified flTF cDNA.

Statistical analyses

Data are indicated as mean ± SEM. Unpaired Student's t-test was performed for comparison of two groups, and two-way ANOVA was used to compare 4 groups of two genotypes and both sexes. For comparison of genotype distributions a X^2-test was applied. A p value <0.05 was considered as significant. Hematology data were analyzed using R-Scripts. Depending on the distribution of the respective data parametric or non-parametric statistical methods were used.

References

1. Rathkolb B, Fuchs H, Gailus-Durner V, Aigner B, Wolf E, Hrabe de Angelis M. Blood Collection from Mice and Hematological Analyses on Mouse Blood. Curr Protoc Mouse Biol. 2013;3(2):101-119.
2. Furlan-Freguia C, Marchese P, Gruber A, Ruggeri ZM, Ruf W. P2X7 receptor signaling contributes to tissue factor-dependent thrombosis in mice. J Clin Invest. 2011;121(7):2932-2944.
3. Rothmeier AS, Marchese P, Petrich BG, et al. Caspase-1-mediated pathway promotes generation of thromboinflammatory microparticles. J Clin Invest. 2015;125(4):1471-1484.

Supplemental Table 1: data table of significantly regulated genes in heart as well as lung tissue from male and female homozygous C213G/C213G TF mice compared to wt TF mice. Data provided as an Excel file.

Supplemental Figure 1

A

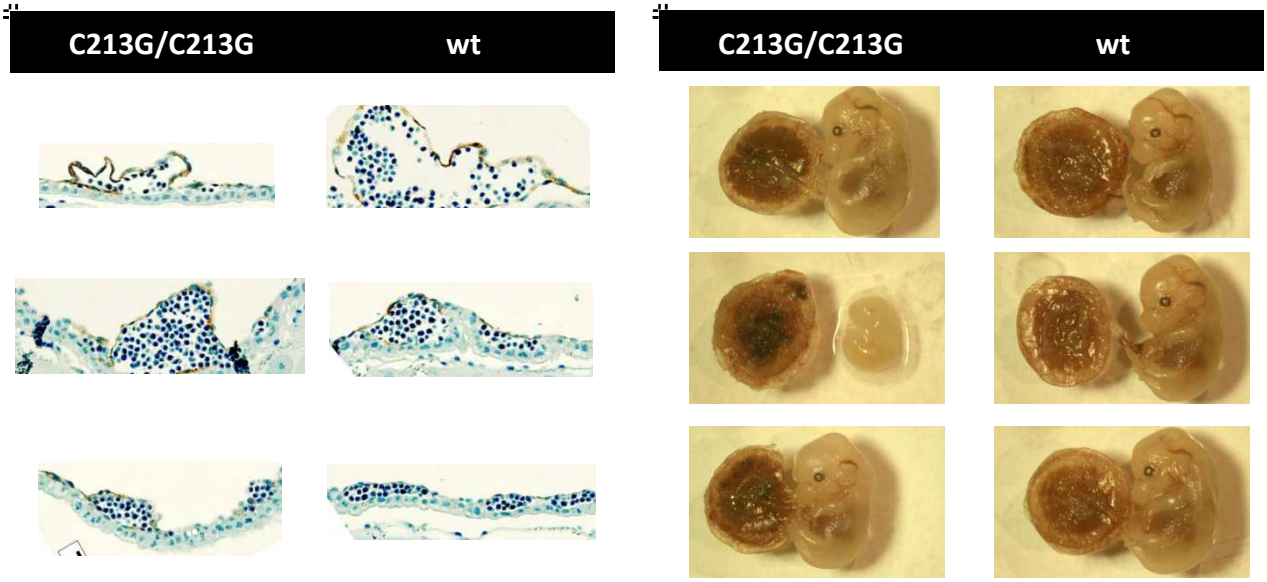

E9.5 yolk sac histology showed similar erythrocyte filling and α-SMA expression in yolk sac vessels of homozygous C213G/C213G TF and wt embryos. At E14.5 dead homozygous C213G/C213G TF embryos were identified. Placentae of homozygous C213G/C213G TF embryos showed various degrees of blood pools. Placentas of 7 wt and 8 C213G/C213G TF mice were examined.

B

	wt		C213G/C213G	
	male	female	male	female
Hemorrhages in heart	0/5	0/5	5/10	7/11
Hemorrhages in lung	1/5	0/5	5/10	1/11
Hemorrhages in brain	0/5	0/5	2/10	2/11

Incidence of organ bleedings in male and female wt and homozygous C213G/C213G TF mice.

Supplemental Figure 2

A

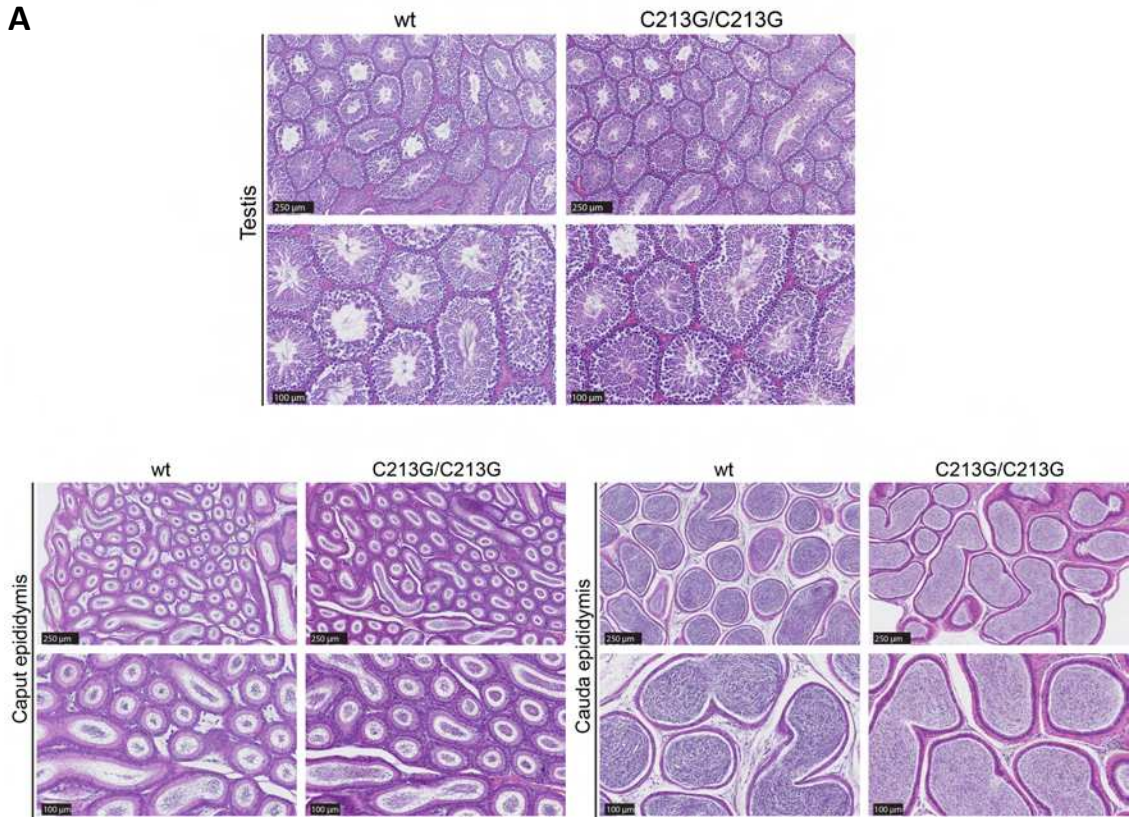

Normal morphology of seminiferous tubules of the testes and sperm density in the epididymides of C213G/C213G TF mice. Representative pictures of hematoxylin and eosin (H&E)-stained sections of (upper panel) testis and (lower panel) epididymis (caput and cauda) from wt and homozygous C213G/C213G TF mice are displayed. 10x (picture above) and 20x (below) magnifications are shown.

B

fITF	**female**		**male**		**ANOVA**	**ANOVA**	**ANOVA**	**Post-Hoc**	**Post-Hoc**
	control	mutant	control	mutant	genotype	sex	genotype : sex	female	male
	n=10	n=10	n=10	n=9					
	mean ± sd	mean ± sd	mean ± sd	mean ± sd	p-value	p-value	p-value	p-value	p-value
Diastolic blood pressure [mm Hg]	125.77 ± 9	116.86 ± 11.5	120.25 ± 15.4	121.95 ± 11.4	0.358	0.955	0.179	0.142	1
Mean arterial pressure [mm Hg]	129.33 ± 8.6	121.3 ± 11.1	124.3 ± 15.2	126.41 ± 11.6	0.442	0.991	0.191	0.176	1
Pulse [bpm]	607.16 ± 33.7	594.18 ± 49.3	596.11 ± 70.8	607.6 ± 34.7	0.963	0.941	0.449	1	1
Systolic blood pressure [mm Hg]	137.38 ± 7.7	131.11 ± 10.7	133.38 ± 15	136.29 ± 12.3	0.657	0.876	0.23	0.304	1

Blood pressure and heart rate. Blood pressure and heart rate are unchanged in homozygous C213G/C213G TF as compared to wt TF mice, irrespective of gender.